

# Bautin bifurcation in a minimal model of immunoediting

Joaquín Delgado\*      Eymard Hernández<sup>†</sup>  
 Lucía Ivonne Hernández-Martínez<sup>‡</sup>

July 4, 2018

## Abstract

One of the simplest model of immune surveillance and neoplasia was proposed by Delisi and Resigno [7]. Later Liu et al [9] proved the existence of non-degenerate Takens-Bogdanov bifurcations defining a surface in the whole set of five positive parameters. In this paper we prove the existence of Bautin bifurcations completing the scenario of possible codimension two bifurcations that occur in this model. We give an interpretation of our results in terms of the three phases immunoediting theory: elimination, equilibrium and escape.

**Key words:** Bautin bifurcation, cancer modeling, immunoediting.

**2000 AMS classification:** Primary: 34C23, 34C60; Secondary: 37G15.

## 1 Introduction

Immune edition conceptualices the development of cancer in three phases [8]. In the first one, formerly known as immune surveillance, the complex of the

---

\*Departamento de Matemáticas, UAM-Iztapalapa Av. San Rafael Atlixco 186, Col. Vicentina, C.P. 09340 CDMX. Email: jdf@xanum.uam.mx

<sup>†</sup>Posgrado en Ciencias Naturales e Ingeniería, UAM-Cuajimalpa. Av. Vasco de Quiroga 4871, Col. Santa Fé Cuajimalpa, C.P. 05348, CDMX. Email: eymardh7@gmail.com

<sup>‡</sup>Universidad Autónoma de la Ciudad de México, Plantel San Lorenzo Tezonco. Calle Prolongación San Isidro 151, Col. San Lorenzo Tezonco, C.P. 09790 CDMX. Email: ivhernandezster@gmail.com

immune system eliminates cancer cells originating from an intrinsic fail in the supresor mechanisms. When some part of cancer cells are eliminated an equilibrium between the immune system and the population of cancer cells is achieved, leading to a durming state. Then the cancer cells accumulate genetic and epigenetic alterations in the DNA that generate specific stress-induced antigens. When a disbalance of the cancer polulation occurs the explosive phase appear with a fast growth of tumor cells. One of the simplest models in the first stage of the immune edition framework, based on a previous model of Bell [3], is due to Delisi and Resigno [7]. They model the population of cancer cells and lymphocytes as a predator–prey system. The cancer tumor grows in the early stage as a spherical tumor that protects the inner cancer cells. Only the cancer cells on the surface of the tumor interact with the lymphocytes. Under proper hypotheses on the balance of the total cancer cells and allometric growth, they propose a model of two ODEs depending on five parameters.

Years after, Liu, Ruan and Zhu [9], study the nonvascularized model of [7] and prove that a Takens-Bogdanov bifurcation of codimension two occurs.

The nonvascularized model of Delisi is

$$\begin{aligned}\frac{dx}{dt} &= -\lambda_1 x + \frac{\alpha_1 x y^{2/3}}{1+x} \left(1 - \frac{x}{x_c}\right), \\ \frac{dy}{dt} &= \lambda_2 y - \frac{\alpha_2 x y^{2/3}}{1+x}\end{aligned}\tag{1}$$

where  $x$  is the number of free lymphocytes that are not bounded to cancer cells,  $y$  is the total number of cancer cells in adimensional variables. The fractional power is the result of assuming an allometric law of the number of cancer cells on the surface of an spherical tumor. Obviously the model is not well suited for  $y = 0$  which correspond to the initial tumor cell being a point. In fact the theorem of uniqueness of solutions does not hold for inital conditions of the form  $(x_0, 0)$ . After a change of variables  $\bar{x} = x$ ,  $\bar{y} = y^{1/3}$ , perform the next reparametrization

$$\frac{dt}{d\bar{t}} = 1 + x,\tag{2}$$

and dropping the bars the system becomes the polynomial system

$$\begin{aligned}\frac{dx}{dt} &= -\lambda_1 x(1+x) + \alpha_1 \left(1 - \frac{x}{x_c}\right) x y^2 \\ \frac{dy}{dt} &= \lambda_2(1+x)y - \alpha_2 x,\end{aligned}\tag{3}$$

Consider  $(x_0, y_0)$  critical point of the system, then

$$y_0 = \frac{\alpha_2 x_0}{\lambda_2(1+x_0)} \quad (4)$$

$$\frac{\lambda_1 \lambda_2^2}{\alpha_1 \alpha_2^2} = \frac{x_0^2(1-x_0/x_c)}{(1+x_0)^3} \quad (5)$$

Therefore the abscissa  $x_0$  of the critical points are determined by the roots of the cubic polynomial (5). In what follows the combination of parameters

$$\psi \equiv \frac{\lambda_1 \lambda_2^2}{\alpha_1 \alpha_2^2}, \quad \lambda = \frac{\lambda_2}{\lambda_1} \quad (6)$$

will be very useful. In particular the critical points can be described by the catastrophe surface

$$\Sigma = \{(\psi, x_c, x_0) \mid x_0^2(1-x_0/x_c) - \psi(1+x_0)^3 = 0\}. \quad (7)$$

in the space of parameters  $\psi$ - $x_c$  and abscissa  $x_0$ . This surface is shown in Figure 1. The plane  $x_0 = 0$  correspond to the trivial critical point  $(0, 0)$  and is a saddle. The red line shows a case of value of the parameters  $(\psi, x_c)$  such that there are three critical points determined by their  $x_0$  abscissa. At a point where the surface folds back, the number of critical point is three, counting the trivial one. The projection of this folding is given by the discriminant of the cubic,

$$\Delta = 4x_c^2 - 27(1+x_c)^2\psi = 0, \quad \text{or} \quad \psi = \frac{4x_c^2}{27(1+x_c)^2}, \quad (8)$$

defines a curve in the parameter plane  $\psi$ - $x_c$  where the projection  $(\psi, x_c, x_0) \mapsto x_0$  restricted to  $\Sigma$  loses range and the catastrophe surface folds back.

The rest of the paper is organized as follows: In section 2 we summarize the results of Liu et al regarding the existence of saddle-node and Takens-Bogdanov bifurcations. In section 3 we state the main result of this paper, the existence of Bautin bifurcations and describe it explicitly in terms of a proper parametrization. We give the main idea of the proof and the details are postponed to the Appendix A. The global bifurcation diagram is completed numerically with MatCont using the local diagrams of the Takens-Bogdanov and Bautin bifurcation as described in the Appendix C. In section 4 we describe the phase portraits derived from the global bifurcation diagram and represented schematically in Figure 3. Finally in Section 5 we give an interpretation of our results. In Appendix C we describe briefly how the numerical continuation with MatCont was performed.

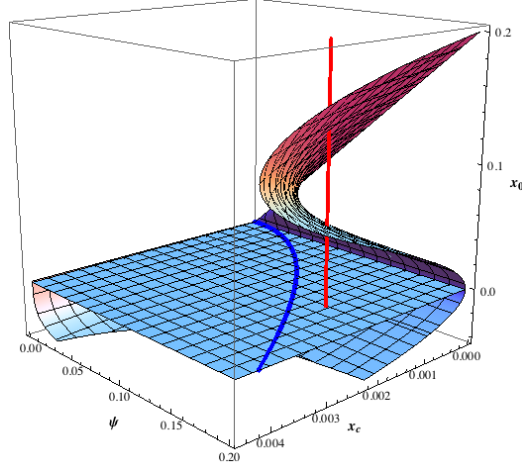


Figure 1: The catastrophe surface in coordinates  $(\psi, x_c, x)$ ,  $x_0$  the abscissa of the critical point. For a given value of  $(\psi, x_c)$  there are up to two critical points with  $x_0 > 0$  and the trivial critical point corresponding to  $x_0 = 0$ . Notice that there are critical points with  $x_0 < 0$  that are not considered. The folding of the surface projects into the saddle–node curve given by (8) in the plane  $\psi$ – $x_c$ .

## 2 Saddle node and Hopf bifurcations

The following two results summarize the results by Liu et al [9].

**Proposition 1** (Liu et al). *The parameter set*

$$SN = \left\{ (\lambda_1, \lambda_2, \alpha_1, \alpha_2, x_c) \mid \psi = \frac{4x_c^2}{27(1+x_c)^2}, \lambda \neq \frac{2(3+x_c)}{3(1+x_c)} \right\}$$

*are saddle node bifurcations of system (3). The phase portrait consists of two hyperbolic and one parabolic sectors.*

Using (8) we can obtain the explicit parametrization of the saddle–node curve in the plane  $\lambda_1$ – $\lambda_2$  for given values of  $\alpha_1$ ,  $\alpha_2$  and  $x_c$ .

$$\lambda_1 = \frac{1}{3} \left( \frac{4x_c^2 \alpha_1 \alpha_2^2 \lambda^2}{(1+x_c)^2} \right)^{1/3}, \quad \lambda_2 = \frac{1}{3} \left( \frac{4x_c^2 \alpha_1 \alpha_2^2}{\lambda(1+x_c)^2} \right)^{1/3}$$

Takens-Bogdanov bifurcations are given as follows:

**Theorem 1** (Liu et al). *The parameter set*

$$BT = \left\{ (\lambda_1, \lambda_2, \alpha_1, \alpha_2, x_c) \mid \psi = \frac{4x_c^2}{27(1+x_c)^2}, \lambda = \frac{2(3+x_c)}{3(1+x_c)} \right\} \quad (9)$$

are non-degenerate Takens-Bogdanov bifurcations of system (3).

For a choice of parameters in  $BT$  the critical point undergoing a BT bifurcation is given by (4) and (5). As a previous construction towards proving our main result, we first characterize the Hopf bifurcations locus.

**Proposition 2.** *The parameter set*

$$H = \{(\lambda_1, \lambda_2, \alpha_1, \alpha_2, x_c) \mid (10) \text{ holds}\}$$

is the Hopf and symmetric saddle bifurcation surface of system (3).

$$0 = (1+x_c)^3\psi\lambda^3 - (\psi x_c^3 + (1-\psi)x_c^2 - 5\psi x_c - 3\psi)\lambda^2 + (x_c^2 + 4x_c + 3)\psi\lambda + (1+x_c)^2(1+x_c\psi)\psi \quad (10)$$

*Proof.* Let  $f, g$  denote the right hand sides in (3), then we look for a common root of the polynomial equations  $f = g = \text{tr}A = 0$ , where  $A = \frac{\partial(f,g)}{\partial(x,y)}$  and  $\text{tr}A = \text{tr}A$ . We compute  $R_1 = \text{Resultant}[\text{tr}A, f, y_0]$ ,  $R_2 = \text{Resultant}[\text{tr}A, g, y_0]$  which are polynomials in  $x_0$ . A necessary condition for  $\text{tr}A = 0 = f$  to have a common root is that  $R_1 = 0$ , and similarly a necessary condition for  $\text{tr}A = g = 0$  to have a common root is that  $R_2 = 0$ . Then compute  $R = \text{Resultant}[R_1, R_2, x_0]$  which is a polynomial in the parameters. A necessary condition for  $R_1 = R_2 = 0$  to have a common root is that  $R = 0$ . If we exclude trivial factors, we end up with (10).  $\square$

Liu et al [9] prove that a non-degenerate Takens-Bogdanov bifurcation occurs for any values of the positive parameters, thus excluding the possibility of codimension three degeneracy. Adam [1] gives sufficient conditions for system (3) to undergo a Hopf bifurcation, although no explicit computation is done. Liu et al describe the Hopf bifurcation locus in terms of parameters involved in the normal form computation, thus not explicit. The expression in Proposition 2 gives an explicit parametrization of the locus of Hopf bifurcations in the parameters.

### 3 Bautin bifurcation

We now give the main idea to compute the first Lyapunov coefficient for a critical point undergoing a Hopf bifurcation. Let  $(x_0, y_0)$  be such a critical point. Then we shift the critical point to the origin  $x = x_0 + \epsilon x_1, y = y_0 + \epsilon y_1$  and expand in powers of  $\epsilon$  in order to collect the homogenous components of the vector field. We first consider the linear part

$$x_1' = ax_1 + bx_1, \quad (11)$$

$$y_1' = cx_1 + dx_1 \quad (12)$$

and perform the linear change of variables  $Y_1 = b_2x_1 - a_2y_1, Y_2 = (a_1b_2 - a_2b_1)x_1$ . Under the hypothesis of complex eigenvalues and the determinant  $a_1b_2 - a_2b_1 > 0$  the system reduces to an oscillator equation  $Y_1' = Y_2, Y_2' = \omega^2 Y_1 - 2\mu Y_1$ , with eigenvalues  $\lambda = \mu \pm \sqrt{\omega^2 - \mu^2}$  and the Hopf condition becomes  $\mu = 0, \omega^2 = a_1b_2 - a_2b_1$ . We compute right and left eigenvectors  $q_0, p_0$  such that  $Aq_0 = i\omega q_0$  and  $A^T p_0 = -i\omega p_0$  and  $\langle p_0, q_0 \rangle = 1$ . Then  $\langle p_0, \bar{q}_0 \rangle = 0$ . Let  $Y = zq_0 + \bar{z}\bar{q}_0$ . Then the whole nonlinear system reduces to (setting  $\epsilon = 1$ )  $z' = \lambda z + G_2(z, \bar{z}) + G_3(z, \bar{z}) + \dots$  then we compute  $\ell_1$  by the formula given by [10, p.309–310].

As shown in the appendix,  $\ell_1$  becomes a polynomial in  $x_0, y_0, \omega$  and after elimination of  $\omega^2$  and  $\omega^4$  which are the only powers appearing there, and of  $y_0$  using (3), a polynomial in  $x_0$  of high degree (19) results. The main difficulty is that computing the abscissa  $x_0$  of the critical point amounts to solving a cubic polynomial. Therefore we compute the resultant of  $\ell_1$  with the cubic polynomial (7) and eliminate  $x_0$ . Taking an appropriate factor of this, we then compute its resultant with the Hopf equation (10). There are two factors. One of this leads to the solution for  $\lambda = \lambda_2/\lambda_1$ ,

$$\lambda = \frac{-3 + x_c}{3(1 + x_c)}$$

Substituting this value in the Hopf equation (10) we solve for  $\psi$  in an appropriate factor. We then get the following

**Theorem 2.** *The parameter set*

$$Bau = \left\{ (\lambda_1, \lambda_2, \alpha_1, \alpha_2, x_c) \mid \psi = \frac{\sqrt{x_c}((-27 + x_c)\sqrt{x_c} + (9 + x_c)^{3/2})}{27(1 + x_c)^2}, \right. \\ \left. \lambda = \frac{-3 + x_c}{3(1 + x_c)} \right\} \quad (13)$$

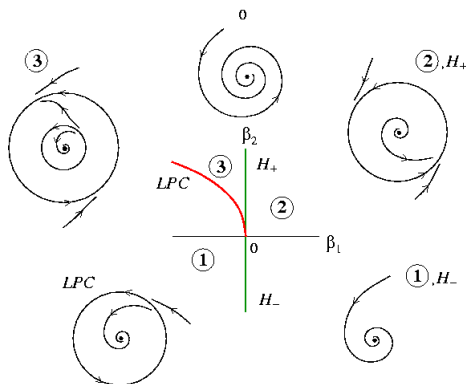


Figure 2: Local diagram of Bautin bifurcation

are Bautin points of codimension 2 of system (3).

### 3.1 Bifurcation diagram around a point of Bautin

The local bifurcation diagram around a Bautin point is shown in Figure 2 (see [10, p.313]) There are two components of the Hopf curve  $H_{\pm}$  corresponding to the sign of the first Lyapunov coefficient  $\ell_0$ . Thus when crossing the component  $H_-$  from positive values of  $\beta_1$  a stable limit cycle appears, and similarly, when crossing the component  $H_+$ , an unstable limit cycle appears. Therefore in the cusp region 3, there coexist two limit cycles the exterior one being stable, the interior one unstable, and both collapse along the LPC curve.

## 4 Global dynamics

Figure 3 shows schematically the bifurcation diagram as computed numerically with MatCont in Figure 10. There are shown three lines of fixed value of  $\lambda_2$  varying  $\lambda_1$ . We will now describe the qualitative phase portrait along these lines. For the upper line  $CT$  corresponding to a value of  $\lambda_2$  just below the Takens–Bogdanov point  $BT$ , the dynamics can be described as follows: In passing from a point  $C$  to a point  $D$  the trivial critical point connects to the saddle point along a heteroclinic orbit. This happens at the point marked as  $K$ . Indeed a curve of heteroclinic connections is depicted along the points  $KK'K''$  although we have not computed it numerically. The transition from  $C$  to  $D$  passing through the heteroclinic connection  $K$ , and further

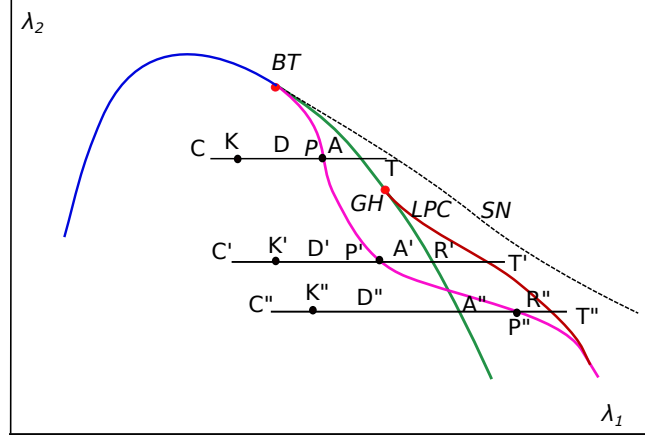


Figure 3: Schema of the bifurcation diagram 2.

evolution to a limit cycle bifurcating from a homoclinic connection at  $P$ , and disappearance of the limit cycle through a transcritical Hopf bifurcation ending at  $T$ , is shown in Figure 4. For completeness we have included the flow at infinity as described in Appendix B. The critical points at infinity  $y = \infty$  are shown as blue points. Notice the hyperbolic sector for  $x = 0$  and the attractor at  $x = x_c$ .

Similarly, the evolution of the phase portrait along the line  $C'T'$  is described in Figure 5. The evolution along the part  $C'K'D'P'A'$  is the same as  $CKDPA$  in Figure 4, the difference is at the further development of an unstable limit cycle inside the stable limit cycle previously created by a homoclinic bifurcation at  $P' = P$ , as shown in figure  $R'$  and further disappearance of both limit cycle as in  $T'$  through a limit point of cycles.

Finally the evolution along the line  $C''T''$  is described as follows: The phase portrait along  $C''K''D''$  is the same as in  $C'K'D'$ . Differently from the previous case, after  $D''$  a Hopf bifurcation occurs and an unstable limit cycle is appear as in  $A''$  and then a second stable limit cycle originating in an homoclinic bifurcation leading to coexistence of two limit cycles as in case  $R'$ . The whole evolution along the line  $C''T''$  is shown in Figure 6 where only the phase portraits different from the previous case are denoted as  $A''$  and  $P''$ ,

Figure 7-(a), (b) shows in detail the evolution along  $C'T'$  in the triangular region of coexistence of two limit cycles, with  $\lambda_1$  as the  $z$ -axis. Notice that along increasing values of  $\lambda_1$ , first a limit cycle bifurcates from a homoclinic an then the second cycle bifurcates from a Hopf point. Figure 7-(c), (d)

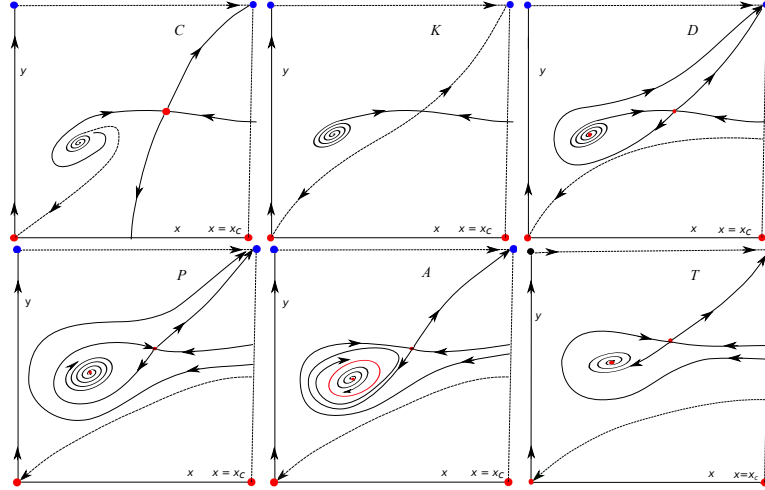


Figure 4: Qualitative phase portrait along the line  $CKDPAT$  of the bifurcation scheme in Figure 3.

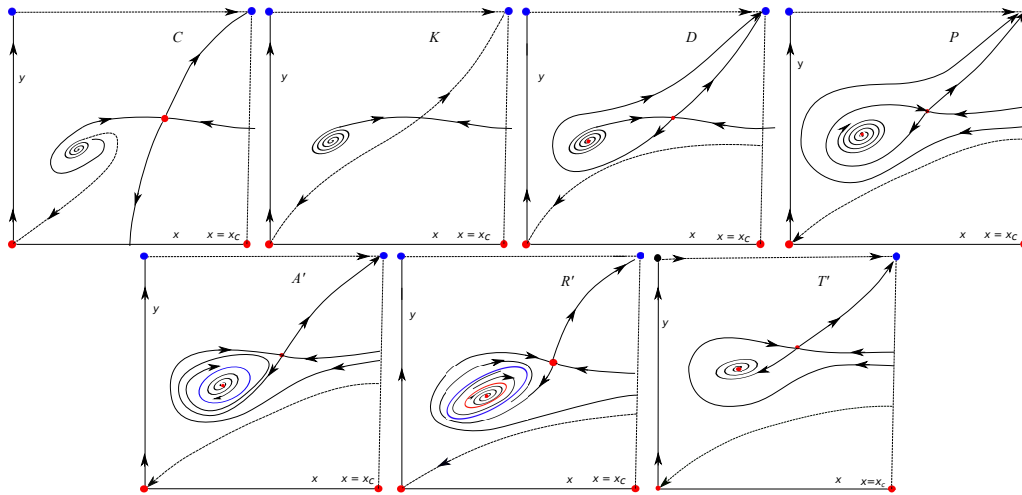


Figure 5: Qualitative phase portrait along the line  $C'K'D'P'A'T'$  of the bifurcation scheme in Figure 3. The phase portrait along the segment  $C'K'D'P'A'$  is the same as  $CKPDA$ .

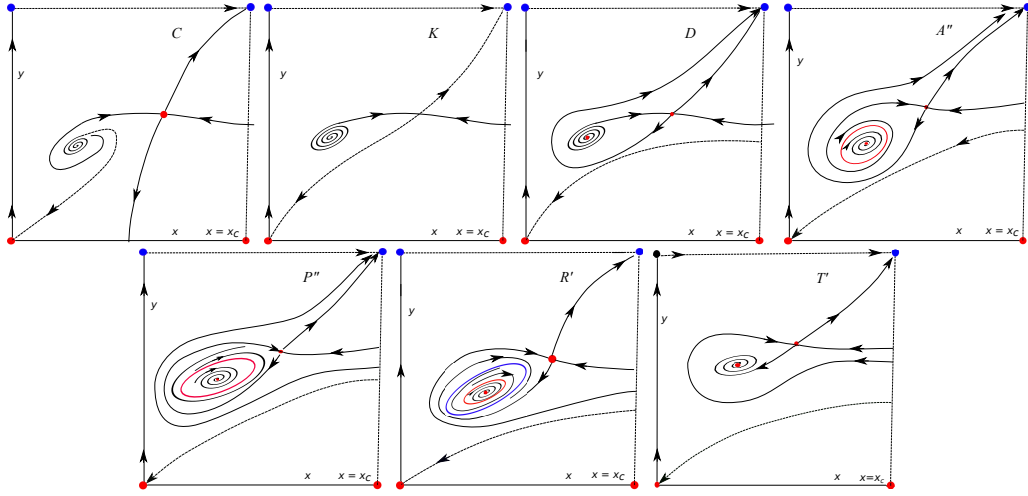


Figure 6: Qualitative phase portrait along the line  $C''K''D''P''A''T''$  of the bifurcation scheme in Figure 3.

evolution along  $C''T''$ .

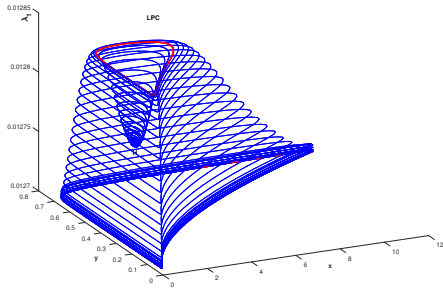
## 5 Implications of the model on the equilibrium phase of immunoediting

In what follows we will be interested on non-negative values of the parameters and  $x$  within the range  $0 < x < x_c$ . Since  $x' < 0$  if  $x = x_c$  and  $y' < 0$  if  $y = 0$ , it follows that the region  $0 < x < x_c$ ,  $0 < y$  is invariant. This delimites the region of real interest (ROI) in the model.

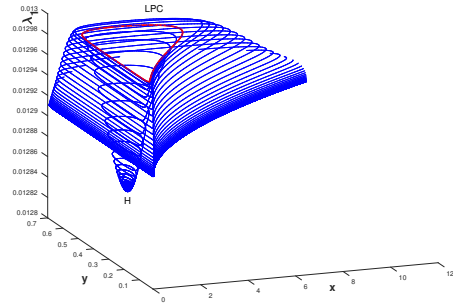
**Proposition 3** (Elimination threshold). *Given  $\alpha_1$ ,  $\alpha_2$ ,  $\lambda_2$ ,  $x_c$ , there exists  $\lambda_1^*$  such that if  $\lambda_1 > \lambda_1^*$ , there exists a curve  $y = h(x)$  such that for any initial condition  $(x_0, y_0)$  such that  $y_0 < h(x_0)$  then there exists  $T > 0$  such that  $y(T) = 0$ .*

*Proof.* Fix  $\alpha_1$ ,  $\alpha_2$ ,  $\lambda_2$  and  $x_c$ . Since the saddle–node curve is the hyperbola  $\lambda_1 \lambda_2^2 = \text{const}$  (see Proposition 1), then for  $\lambda_1$  large enough the unique critical point is the origin and is a saddle with the positive  $y$  axis as a branch of the unstable manifold. Let us consider the rectangular region within the ROI

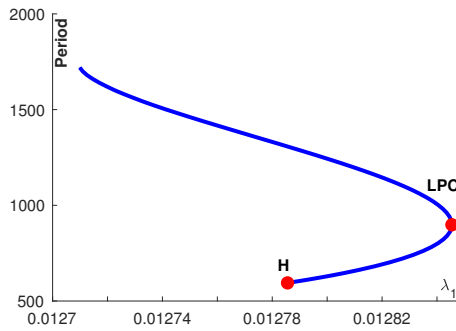
$$R = \{(x, y) \mid 0 < x < x_c, \quad 0 < y < k\}$$



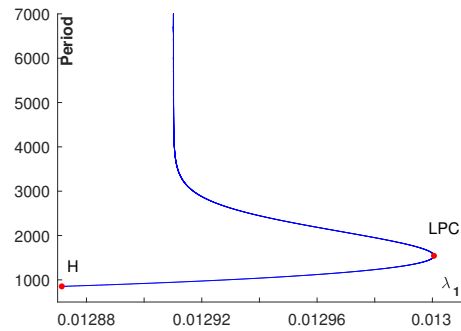
(a) Numerical continuation of limit cycles in coordinates  $(x, y, \lambda_1)$  along the line  $C'T'$  within the region of coexistence of two limit cycles.



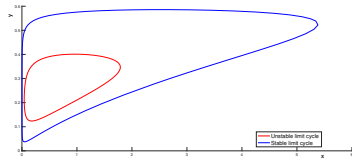
(b) Numerical continuation of limit cycles in coordinates  $(x, y, \lambda_1)$  along the line  $C''T''$  within the region of coexistence of two limit cycles.



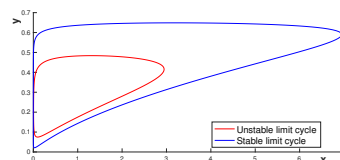
(c) Parameter  $\lambda_1$  versus period  $T$  of the cycles.



(d) Parameter  $\lambda_1$  versus period  $T$  of the cycles.



(e) Two limit cycles for the same  $\lambda_1$  parameter value.



(f) Two limit cycles for the same  $\lambda_1$  parameter value.

Figure 7: Coexistence of two limit cycles along the line  $C'T'$ : (a), (c) and (b). Along the line  $C''T''$ : (b), (d) and (f).

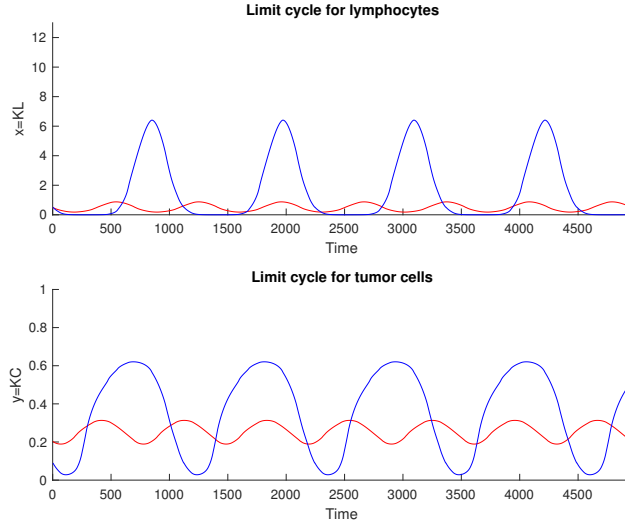


Figure 8: Graphs of coexisting limit cycles of Figure 7. Stable in blue, unstable in red.

We have seen that on the boundary  $x = x_c$ ,  $x' < 0$ ; on the boundary  $y = 0$ ,  $y' < 0$ . On the upper boundary  $y = k$ . Since  $x$  remains bounded, it follows that  $y' = \lambda_2 y(1 + x) - \alpha_2 x$  is positive for  $y = k$  large enough. We now follow the unstable manifold  $W^s(0, 0)$  backwards in time. A straightforward computation of the stable eigenvalue shows that a small component of  $W^s(0, 0)$  belongs to  $R$ , since there are no critical points within  $R$  it follows that it must intersect the line  $x = x_c$ . It remains to show that in fact the component of  $W^s(0, 0)$  within the region  $0 < x < x_c$  can be expressed as the graph of a function  $y = h(x)$ . Now from the first equation  $x' = -\lambda_1 x(1 + x) + \alpha_1 x(1 - x/x_c)y^2$ , since  $x, y$  remain bounded and  $\lambda_1$  is large enough, it follows that  $x' < 0$ , and the result follows.  $\square$

The above theorem defines a threshold value of the population of cancer cells  $y_c$  given by the intersection of  $W^s(0, 0)$  and the line  $x = x_c$ , namely  $y_c = h(x_c)$ : let  $y_0$  be an initial population of cancer cells  $y_0 < y_c$ , for a given growth parameter  $\lambda_2$  and interaction constants  $\alpha_{1,2}$  then there exists  $x_0 = h^{-1}(y_0)$  such that for  $x'_0 > x_0$  the evolution of cancer cells  $y(t)$  with initial condition  $(x'_0, y_0)$  becomes zero. Geometrically, the horizontal line

$y = y_0$  in phase space intersects the graph of the curve  $y = h(x)$  at a point  $(\bar{x}_0, \bar{y}_0)$  and for an initial population of lymphocytes large enough  $x_0 < x'_0 < x_c$ , the solution with initial condition  $(x'_0, y_0)$  crosses the line  $y = 0$  for some finite time  $T$  and  $y(T) = 0$ . See Figure 9

Notice that the above dynamics occurs in the scaled variables  $(x, y)$ , The branch of the stable manifold  $y = h(x)$  transforms back to the original variables  $(x, \bar{y})$  into a curve  $\bar{y} = h(x)^3$  however, in the original variables the locus  $\bar{y} = 0$  does not make sense for two reasons: the first one is that the model breaks down because of the hypothesis of a spherical tumor. The second is that the system (1) is not Lipschitz for  $\bar{y} = 0$ . Indeed one expects non-uniqueness as in the well known example  $\bar{y}' = \bar{y}^{2/3}$ . Nevertheless the threshold curve is still defined in the original variables  $(x, \bar{y})$ , and since the change of variables is  $C^1$  outside this singular locus  $\bar{y} = 0$ , the same dynamical behaviour occurs in the non-scaled variables.

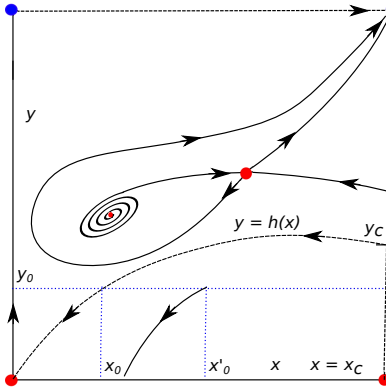


Figure 9: Illustration of Threshold Theorem

According to the immune edition theory the relation between tumor cells and the immune system is made up of three phases (commonly known as the three E's of cancer): elimination, equilibrium and escape [6]. Not in these terminology though, Delisi and Resigno [7], describe these phases in terms of regions delimited by the zeroclines. For example the authors mention that within the region  $x' < 0, y' > 0$  denote by  $A$  in [7] solution evolves eventually to escape to  $x = x_c, y = \infty$ . According to the Threshold Theorem 9, this is true for initial conditions above the curve  $y = h(x)$ . Here we describe in more detail the three phases according to the regions delimited by the invariant manifold and basins of attraction. For example, the elimination phase is

described as the region below the threshold curve; the explosive phase as the basin of attraction of the point at infinity obtained by the compactification of phase space along the  $y$  direction (see Appendix B). The equilibrium phase are the basins of attraction of either a stable anti-saddle or a stable limit cycle.

The existence of a Bautin bifurcation and the global bifurcation diagram continued numerically, implies the existence of a triangular region in the plane of parameters  $\lambda_1$ - $\lambda_2$ , for fixed values of  $\alpha_1$ ,  $\alpha_2$  and  $x_c$  as shown in Figure 10. Within this region two limit cycles exist and the detailed analysis of the phase diagrams along the lines  $CT$ ,  $C'T'$  and  $C''T''$  in Figure 3 and explained in the text, leads to the conclusion that the inner limit cycle is unstable and the exterior one is stable. These two limit cycles are shown in Figure 7, the corresponding plots against the time are shown in Figure 8. This implies that for an initial condition within the interior of the inner limit cycle, the solution tends asymptotically to the values of the stable equilibrium. This would correspond to the equilibrium phase in the immunoedition theory. Meanwhile for an initial condition just outside the unstable inner cycle, the population of cancer cells and lymphocytes grow in amplitude and tends towards a periodic state but of larger amplitude. This yields a new type of qualitative behaviour predicted by the model.

Escape phase in the immunoedition theory corresponds to the basin of attraction of the point at infinity  $x = x_c$ ,  $y = +\infty$ . The analysis in Appendix B shows that this point is stable, so there is an open set of initial conditions leading to the escape phase. The basin of attraction of the point at infinity is delimited first by the threshold curve, and secondly by the unstable manifolds of the saddle point with positive coordinates here denoted as  $(x_s, y_s)$ . The structure of its stable and unstable branches delimits three types of behavior leading to escape. In the first one, for an initial condition  $x_0 > x_s$  and  $y_0$  large enough, there is a transitory evolution of diminishing values of cancer cells  $x(t)$  less than  $x_s$  but finally leading to escape. This region is delimited by the unstable branch connecting  $(x_s, y_s)$  and the point at infinity and the stable branch crossing the line  $x = x_c$ . The second type of evolution leading to escape occurs for an initial condition of large values of initial population of lymphocytes  $x_0$  with a great diminishing of  $x(t)$ , namely less than  $x_a$ , the abscissa of the anti-saddle critical point  $(x_a, y_a)$ , following an increase of cancer cells and lymphocytes leading finally to escape. This kind of solutions can be described as a turn around the anti-saddle before escaping. A third and more complex behaviour occurs when the initial condition lies on the boundary of

the basin of attraction of a limit cycle. In this situation a small perturbation can lead to oscillations of increasing magnitude and finally to escape.

## A Computation of the first Lyapunov exponent

In this section we present the main procedure to compute of the first Lyapunov exponent at a Hopf point.

Let  $(x_0, y_0)$  be a critical point. Replacing  $x = x_0 + x_1$ ,  $y = y_0 + y_1$  in (3),

$$\begin{aligned}\frac{dx_1}{dt} &= -\lambda_1(x_0 + x_1)(1 + x_0 + x_1) + \alpha_1 \left(1 - \frac{x_0 + x_1}{x_c}\right) (x_0 + x_1)(y_0 + y_1)^2 \\ \frac{dy_1}{dt} &= \lambda_2(y_0 + y_1)(1 + x_0 + x_1) - \alpha_2(x_0 + x_1),\end{aligned}$$

and expanding we have

$$\begin{aligned}x_1' &= a_0 + a_1x_1 + a_2y_1 + a_3x_1^2 + a_4y_1^2 + a_5x_1y_1 + a_6x_1y_1^2 + a_7x_1^2y_1 + a_8x_1^2y_1^2 \\ y_1' &= b_0 + b_1x_1 + b_2y_1 + b_3x_1y_1,\end{aligned}\tag{14}$$

where

$$\begin{aligned}a_0 &= -\lambda_1x_0(1 + x_0) + \alpha_1 \left(1 - \frac{x_0}{x_c}\right) x_0y_0^2, \\ b_0 &= \lambda_2y_0(1 + x_0) - \alpha_2x_0.\end{aligned}$$

Of course  $a_0 = b_0$  yields the equations for the critical points. The rest of the coefficients are

$$\begin{aligned}a_1 &= -\lambda(1 + 2x_0) + \alpha_1 \left(1 - \frac{2x_0}{x_c}\right) y_0^2, & a_2 &= 2\alpha_1x_0y_0 \left(1 - \frac{x_0}{x_c}\right), \\ a_3 &= -\lambda_1 - \frac{\alpha_1y_0^2}{x_c}, & a_4 &= \alpha_1x_0 \left(1 - \frac{x_0}{x_c}\right), \\ a_5 &= 2\alpha_1y_0 \left(1 - \frac{2x_0}{x_c}\right), & a_6 &= \alpha_1 \left(1 - \frac{2x_0}{x_c}\right), \\ a_7 &= -2\frac{\alpha_1y_0}{x_c}, & a_8 &= -\frac{\alpha_1}{x_c}, \\ b_1 &= \lambda_2y_0 - \alpha_2, & b_2 &= \lambda_2(1 + x_0), \\ b_3 &= \lambda_2.\end{aligned}$$

Consider the linear part  $x' = Ax$  where  $x = (x_1, y_1)^T$  and

$$A = \begin{pmatrix} a_1 & a_2 \\ b_1 & b_2 \end{pmatrix}$$

Perform the linear change of coordinates

$$Y = Mx, \tag{15}$$

where  $Y = (Y_1, Y_2)^T$  and

$$M = \begin{pmatrix} b_2 & -a_2 \\ a_1 b_2 - a_2 b_1 & 0 \end{pmatrix}$$

then the linear system is transformed into

$$Y' = RY, \quad R = \begin{pmatrix} 0 & 1 \\ -\det(A) & \text{tr}(A) \end{pmatrix}$$

Then  $R$  has the canonical form

$$R = \begin{pmatrix} 0 & 1 \\ -\omega^2 & 2\mu \end{pmatrix}$$

where we have supposed and set that  $0 < \det(A) \equiv \omega^2$ ,  $\text{tr}(A) = 2\mu$  and  $\mu^2 - \omega^2 < 0$  so we have complex eigenvalues  $\lambda = \mu \pm i\sqrt{\omega^2 - \mu^2}$ ,

Let us consider that the real part of the eigenvalues is zero ( $\mu = 0$ ), then

$$R_0 = \begin{pmatrix} 0 & 1 \\ -\omega^2 & 0 \end{pmatrix},$$

and we want to find vectors  $q_0$  y  $p_0$ , such that  $R_0 q_0 = i\omega q_0$ ,  $R_0^T p_0 = -i\omega p_0$ ,  $\langle p_0, q_0 \rangle = 1$  and  $\langle p_0, \bar{q}_0 \rangle = 0$ . We find

$$q_0 = \frac{1}{2i\omega} \begin{pmatrix} 1 \\ i\omega \end{pmatrix}$$

and

$$p_0 = \begin{pmatrix} -i\omega \\ 1 \end{pmatrix}.$$

Let us transform the complete system (14) at a critical point with complex eigenvalues  $\lambda \pm i\omega$

$$x' = Ax + H_2(x) + H_3(x) + \dots,$$

by means of the change of variables (15) then

$$\begin{aligned}
Y' &= Mx' \\
&= MA_0x + MH_2(x) + MH_3(x) + \dots, \\
&= MA_0(M^{-1}Y) + MH_2(M^{-1}Y) + MH_3(M^{-1}Y) + \dots \\
&= R \begin{pmatrix} Y_1 \\ Y_2 \end{pmatrix} + K_2 \begin{pmatrix} Y_1 \\ Y_2 \end{pmatrix} + K_3 \begin{pmatrix} Y_1 \\ Y_2 \end{pmatrix} + \dots
\end{aligned}$$

where  $K_l = MH_lM^{-1}$ , for  $l = 1, 2, \dots$

Now introduce the complex variable  $z$  by

$$\begin{pmatrix} Y_1 \\ Y_2 \end{pmatrix} = zq_0 + \bar{z}\bar{q}_0,$$

then system is reduced to the normal form

$$\begin{aligned}
z' &= \lambda z + \langle p_0, K_2(zq_0 + \bar{z}\bar{q}_0) \rangle + \dots \\
&= \lambda z + G_2(z, \bar{z}) + G_3(z, \bar{z}) + \dots \\
&= \lambda z + \frac{g_{20}}{2}z^2 + g_{11}z\bar{z} + \frac{g_{02}}{2}\bar{z}^2 + \dots
\end{aligned}$$

where

$$G_l = \langle p_0, K_l(zq_0 + \bar{z}\bar{q}_0) \rangle, \quad l = 2, 3 \dots$$

and  $g_{ij} = \frac{1}{i!j!} \frac{\partial G_l}{\partial z^i \partial \bar{z}^j}$ , for  $i, j = 0, 1, \dots$ . We will need the expansion up to third order terms, in particular the coefficient  $g_{11}$  at the third order

We will compute the first Lyapunov coefficients using the formulas (3.18) in [10] for the coefficient  $c_1(0)$  of the Poincaré normal form and

$$\ell_1(0) = \frac{\text{Re}(c_1(0))}{\omega} \tag{16}$$

where

$$c_1(0) = \frac{g_{21}}{2} + \frac{g_{20}g_{11}i\omega}{2\omega^2} - i\frac{g_{11}g_{11}}{\omega} - i\frac{g_{02}g_{02}}{6\omega}$$

Observe that the change of coordinates (15) contains the coordinates of the critical point  $(x_0, y_0)$  and so the coefficients  $g_{ij}$ . Therefore, we have to impose on the formal expression we get using (16) from the coefficients  $g_{ij}$  up to third order, the restriction of a critical point, with zero real part and positive determinant equal to  $\omega^2$ . We achieve this as follows: The expression (16) is a polynomial expression depending on  $(x_0, y_0)$  and the parameters

$P(x_0, y_0, \lambda_1, \lambda_2, x_c, \alpha_1, \alpha_2)$ . Firstly we eliminate  $y_0$  using (4) obtaining a polynomial expression in  $x_0$  of order 19 and the parameters and still denote by  $P(x_0, \lambda_1, \lambda_2, x_c, \alpha_1, \alpha_2)$ . The abscissa  $x_0$  of the critical point satisfy the cubic equation (5) written here as  $Q(x_0, \lambda, \psi, x_c)$ . Suprisingly, the coefficients of  $P$  and  $Q$  can be expressed solely in terms of the combination of parameters  $\lambda$ ,  $\psi$  and  $x_c$ . Next we eliminate  $x_0$  using the resultant

$$R_1(\lambda, \psi, x_c) = \text{Resultant}(P(x_0, \lambda, \psi, x_c), Q(x_0, \lambda, \psi, x_c), x_0).$$

Also the Hopf surface can be expressed in terms of the same combination of parameters as shown in (10) as  $R_2(\lambda, \psi, x_c) = 0$ , then we compute

$$R_3(\lambda, x_c) = \text{Resultant}(R_1(\lambda, \psi, x_c), R_2(\lambda, \psi, x_c), \psi)$$

and we get from a non trivial factor of  $R_3$

$$\lambda = \frac{-3 + x_c}{3(1 + x_c)} \quad (17)$$

Finally, substituting (17) in the Hopf surface  $R_2(\lambda, \psi, x_c) = 0$  we get the nonnegative solution

$$\psi = \frac{\sqrt{x_c} ((-27 + x_c)\sqrt{x_c} + (9 + x_c)^{3/2})}{27(1 + x_c)^2}.$$

## B Blow up of infinity

In order to study solutions that escape to infinity in the direction  $y \rightarrow \infty$  we perform a blow up of infinity by the change of variables  $(x, y) \mapsto (x, v = x/y)$ , a further rescaling of time  $dt/dt' = v^2$  extends the system up to  $v = 0$  corresponding to infinity  $y = \infty$ ,  $x > 0$  (3)

$$\begin{aligned} \frac{dx}{dt'} &= -\lambda_1 x(1+x)v^2 + \alpha_1 x^3 \left(1 - \frac{x}{x_c}\right), \\ \frac{dy}{dt'} &= vx \left(\alpha_1 x \left(1 - \frac{x}{x_c}\right) - \lambda_2\right) + \alpha_2 v^2 - v^3(\lambda_1(1+x) + \lambda_2). \end{aligned} \quad (18)$$

We see that  $v = 0$  becomes invariant and the reduced system at infinity is

$$\frac{dx}{dt'} = x^3(1-x)$$

showing that along  $v = 0$ ,  $x > 0$ ,  $x = x_c$  an attractor.

To determine the local phase portrait of system (18) at the critical point  $x = x_c, v = 0$ , we compute its linearization

$$A = \begin{pmatrix} -x_c^2 \alpha_1 & 0 \\ 0 & -x_c \lambda_2 \end{pmatrix}$$

thus  $(x_c, v = 0)$  is an attractor. The origin  $x = 0 = v$  is also a degenerate critical point with zero linear part with terms of third order the least. Performing a radial blow using polar coordinates  $x = r \cos \theta$ ,  $v = r \sin \theta$  we get

$$\begin{aligned} \frac{dr}{dt} &= r(-\lambda_1 + \alpha_1 \cot^2 \theta - \lambda_2 \sin^2 \theta) + \\ &\quad r^2 \left( -\lambda_1 \cos^2 \theta + \alpha_2 \sin^3 \theta - \frac{\alpha_1}{x_c} \cot^2 \theta - (\lambda_1 + \lambda_2) \cos \theta \sin^2 \theta \right) \\ \frac{d\theta}{dt} &= -\lambda_2 \cos \theta \sin \theta - r \cos \theta \sin \theta (\lambda_2 \cos \theta - \alpha_2 \sin \theta) \end{aligned}$$

which shows that  $r = 0$ ,  $0 < \theta < \pi/2$  is invariant. Setting  $r = 0$  we get

$$\frac{d\theta}{dt} = -\lambda_2 \cos \theta \sin \theta$$

which is always negative for  $0 < \theta < \pi/2$ . Thus the origin is a degenerate critical point with a hyperbolic sector.

## C Numerical continuation

Following [9] we take the numerical values

$$\lambda_1 = 0.01, \lambda_2 = 0.006672, \alpha_1 = 0.297312, \alpha_2 = 0.00318, x_c = 2500$$

satisfying conditions (3) for a BT bifurcation, and the coordinates  $x_0 = 1.9976$ ,  $y_0 = 0.317619$  for the critical point, according to (4), (5). Figure 10 (a)–(b) shows the family of homoclinic connections in phase space, originating from the BT critical point. Since continuing the family of homoclinics from the BT point sometimes is difficult (see [2]), for the computation of the initial member of the family of homoclinics we use the homotopy method near the previous values of  $\lambda_1$ ,  $\lambda_2$  and then continue forward and

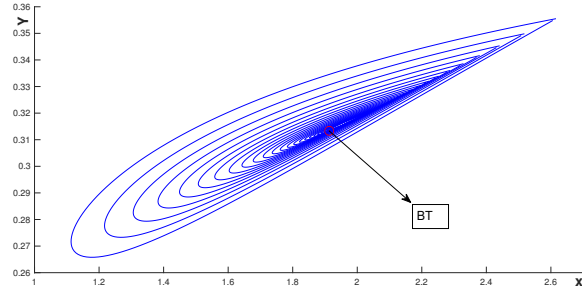
backward to assure that the family originates from the BT point. The curve of homoclinics is shown in Figure 10 as the violet curve. The Bautin point (GH) is detected by continuing the Hopf curve from the BT point.

The Delisi model diagram bifurcation is shown in Figure 10 (b). The saddle-node bifurcation curve is shown in black, the green corresponds to the Hopf bifurcation, the curve in red corresponds to the saddle-node bifurcation of periodic orbits (limit point of cycles) and the blue one to symmetric saddles.

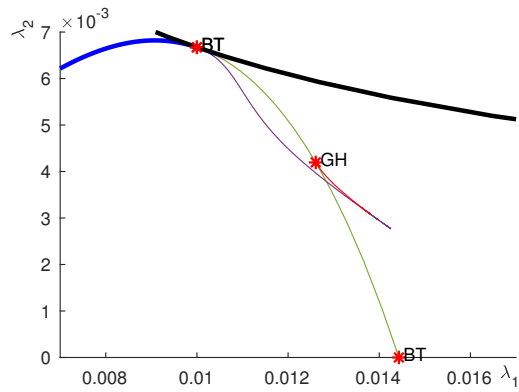
## References

- [1] Adam J. A. Effects of vascularization on lymphocyte/tumor cell dynamics: Qualitative features. *Math. Comput. Modelling*, Elsevier Science Ltd., **23**, No. 6, 1–10, 1996.
- [2] Al-Hdaibat B., Govaerts, W., Kuznetsov, Y.A. and Meijer, H.G.E. Initialization of Homoclinic Solutions near Bogdanov–Takens Points: Lindstedt–Poincaré Compared with Regular Perturbation Method. *SIAM J. Applied dynamical systems*, Society for Industrial and Applied Mathematics, **15**, No. 2, 952–980, 2016.
- [3] Bell, G.I. Predator–prey simulating an immune response. *Mathematical Biosciences* **16**, 291–314, 1973.
- [4] Beyn W. J. Numerical analysis of homoclinic orbits emanating from a Takens-Bogdanov point. *IMA Journal of Numerical Analysis*, **14**, 381–410, 1994.
- [5] Champneys A. R. and Kuznetsov Yu. A. Numerical detection and continuation of codimension–two homoclinic bifurcation. *International Journal of Bifurcation and Chaos*, **4**, No. 4, 785–822, 1994.
- [6] Dunn, G.P, Old, L.J. and Schreiber, R.D. The three ES of Cancer Immunoediting. *Annual Review of Immunology*, **22**, 329–360, 2004.
- [7] DeLisi C. and Rescigno, A. Immune surveillance and neoplasia-I. A minimal mathematical model. *Bull. Math. Bio.*, **39**, 201–221, 1977.
- [8] Kim, R., Emi, M. and Tanab, K. Cancer immunoediting from immune surveillance to immune escape. *Immunology*, **21**, 11–14, 2007.

- [9] Liu, D., Ruan, S. and Zhu, D. Bifurcation analysis in models of tumor and immune system interactions. *Discrete and continuous dynamical systems series B.*, **12**, No. 1, 2009.
- [10] Kuznetsov, Y.A *Elements of Applied Bifurcation Theory*, second edition, Springer, 1998.



(a) Continuation of the homoclinic orbit of avascular Delisi model (3) near Bogdanov-Takens bifurcation.



(b) Bifurcations of avascular Delisi model (3) from parameters values  $\alpha_1 = 0.297312$ ,  $\alpha_2 = 0.00318$  and  $x_c = 2500$ .

Figure 10: Numerical continuation of bifurcation diagram with MatCont. Saddle-node: black; Hopf: green; limit point of cycles: red; symmetric saddles: blue; homoclinic: violet.